Towards a single-molecule FRET study of Frauenfelder's nonexponential rebinding of CO in myoglobin

Eskandari Alughare, Z.

4

FRET study of CO binding to fluorescently labeled myoglobin

Based on the estimated quantum yield of bond breaking in the chapter 3, we believe that the MbCO complex should be stable enough to monitor FRET from the near infra-red donor to the heme group, with enough donor fluorescence photons being emitted before photodissociation of the MbCO occurs. The FRET measurement of the donor fluorescence intensity of fluorescence lifetime.
In this chapter, our aim is to prepare a properly labeled MbCO with a dye that can be excited and emits in the near infra-red, and to study the energy transfer from the dye to Mb and to MbCO when illuminating with λ > 700 nm. Would it be possible to distinguish between the two Mb states; MbCO and deoxy-Mb, and to use this fluorescence signal to study the kinetics of CO rebinding?

4.1 Introduction

Fluorescence spectroscopy is a reliable method for detecting the activity of proteins . [1,2] The single-molecule FRET (smFRET) approach has been widely used to determine kinetic rates of proteins. [3-4] Proteins can be specifically labeled using one or more dyes for smFRET measurements. For example, as I discussed in chapter 3, azurin is a redox protein which has a redox cofactor copper atom to carry out specific redox reactions. The absorption spectrum of azurin changes when the redox state of the prosthetic group changes ($Cu^{+} \leftrightarrow Cu^{2+}$). Therefore, the attachment of a fluorescent molecule to the protein surface makes it possible to monitor the fluorescence emission of single-dye-labeled azurin molecules by means of Förster Resonance Energy Transfer (FRET) spectroscopy. [5]

Inspired by the FRET-based probing of the redox state of azurin, we explore whether the kinetics ligand to binding to myoglobin (Mb) could be measured using FRET. In the case of Mb a change of the absorption spectrum is observed when CO binds to or dissociates from the heme. Thus, by labeling Mb with the proper dye, we can monitor the fluorescence emission of the dye-labeled-Mb in different states by mean of Förster Resonance Energy Transfer (FRET). In this way, we hope to determine the rebinding kinetics of CO at the single-molecule level.

In Chapter 2, we showed that the Mb spectrum consists of three main parts: the Soret band (300-500 nm), the Q-band(s) (500-700 nm) and the NIR bands (700-1000 nm). When the Mb-CO bond is illuminated in the area of the Soret band or the Q-band, the quantum yield of breaking the Mb-CO bond is unity. Therefore, monitoring the absorption spectrum of a single molecule in those spectral ranges would unavoidably lead to CO dissociation and could not be used for monitoring CO binding. What about the NIR spectral range? The interesting question is whether illumination with near infra-red light with a wavelength beyond 700 nm breaks the MbCO bond or not and if yes, with which photodissociation quantum yield?. And answer this question whether FRET to MbCO will dissociate the bond when measured in the near infra-red region. In chapter 3, we described experiments to determine the quantum yield of photodissociation under near infra-red illumination in order to determine if that region can be used for FRET. We proposed in chapter 3 an approach using a weak band beyond 700 nm (band III at 760 nm) in the deoxy-Mb absorption spectrum to quench the fluorescence of a dye donor fluorescing in the near infar-red range. As band III is absent from the spectrum of MbCO, breakage of the CO bond due to resonant energy transfer from the excited dye to the heme excited states seemed unlikely, but this has to be checked. Although the absorption coefficient of Band (III) is very small, however, as the Forster radius; R_0 depends on the sixth root (eq. 4.1), make it possible to use this system for FRET study by control of the distance between the donor and acceptor. Our results of chapter 3 show that illumination of MbCO with near infra-red light (700-800 nm) does not break the Mb-CO bond efficiently. Based on the estimated quantum yield of bond breaking, we believe that the MbCO complex should be stable enough to monitor FRET from the near infra-red donor to the heme, with enough donor fluorescence photons emitted before dissociating MbCO during the FRET measurement. Although lifetime measurements are more sensitive than the fluorescence intensity, our FRET study is based on the both fluorescent intensity and lifetime measurement.

In this chapter, our aim is to prepare a properly labeled MbCO with a dye that can be excited and which emits in the near infra-red, and to study the energy transfer from the dye to Mb and to MbCO when illuminating with $\lambda > 700$ nm. Would it be possible

to distinguish between two Mb states; MbCO and deoxy-Mb, and to use this fluorescence signal to study the kinetics of CO rebinding?
It should be noted that this chapter focuses on the FRET study of labeled MbCO at room temperature. However, to study the kinetic rebinding of CO to myoglobin at low temperature, in future, it is essential to measure absorption spectra of MbCO and deoxy-Mb in near infra-red region at low temperature (120-140 K) because the absorption spectra in particular absorption spectrum of deoxy-Mb will change when the temperature decreased. [6]

4.1.1 Can we measure the FRET efficiency of different states of labeled Mb (deoxy-Mb and MbCO)?

In FRET, energy transfer occurs from a donor fluorophore to an acceptor molecule, by which the fluorescence emission of the donor is quenched and the fluorescence of the acceptor is sensitized. In some metallo-proteins, the donor can be a fluorescent dye attached to a specific site of the protein, whereas the acceptor can be a center inside the protein such as the redox copper center in azurin or the heme in Mb. As the heme in Mb displays several electronic absorption bands between 350 and 1000 nm, it can act as an acceptor for a fluorescent dye attached to Mb. The FRET efficiency is sensitive to the position of the dye with respect to the heme. The smaller the distance to the heme, the more efficient the energy transfer. Moreover, the larger the spectral overlap between the absorption spectrum of the Mb and the emission spectrum of the donor dye, the stronger the energy transfer from dye to heme. The FRET efficiency can be quantified by fluorescence intensity or, more reliably, by the fluorescence lifetime of the donor dye.
The two relevant states of Mb, deoxy-Mb and MbCO, have very different absorption spectra in the near infra-red spectral range (700-1000 nm) (Figure 4.1). Therefore, the FRET efficiency for dye labeled-deoxy-Mb must be different from that of the dye-labeled-MbCO. However, The FRET efficiency difference between deoxy-Mb and MbCO has to be large enough to be readily observable on the fluorescence intensity and/or lifetime.

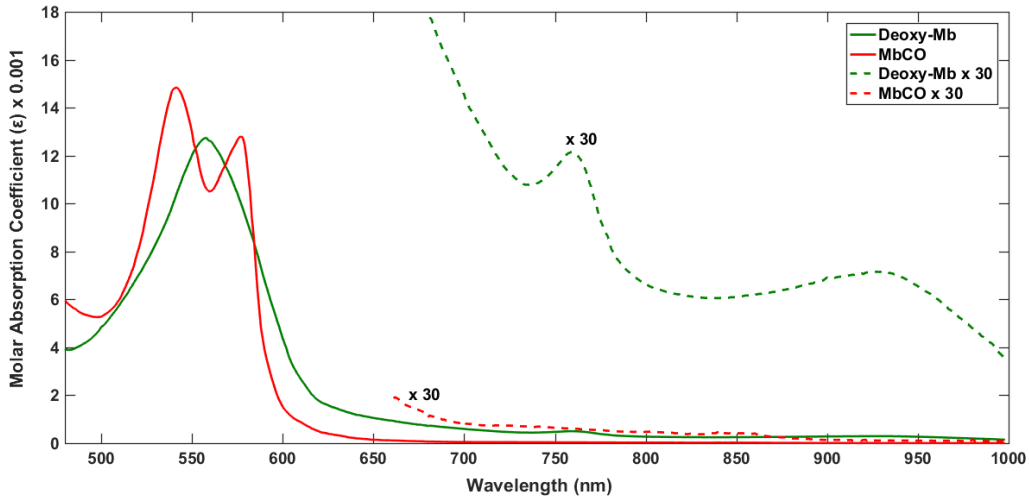

Figure 4.1 *Absorption spectrum of the Q-bands (500-700 nm) and NIR bands (700-1000 nm) for two Mb states: deoxy-Mb (green), and MbCO (red) from horse heart Mb at room temperature, in Sørensen's phosphate buffer (0.05 mM) with pH 6.8-8. The stippled lines represent the 30x enlarged spectra.* [7]

4.1.2 Investigating rebinding kinetics of CO to Mb with FRET

FRET strategies are often used to investigate molecular interactions when the distance between partners is 1-10 nm, for example between a donor (dye label on a protein) and an acceptor (heme in Mb).
The FRET efficiency is related to fluorescence lifetime, and additional information can be extracted by analyzing the fluorescence intensity and lifetime together. Time-dependent FRET measurements have been developed to characterize the reaction kinetics of enzymes [8,9] and ligand-receptor interactions. [10] Fluorescence lifetime correlation analyses have also been used to distinguish different species in a mixture [11] or to probe fast molecular processes on the microsecond to millisecond time scale. [12] Importantly, different species can be more reliably identified by analyzing the lifetime data than by analyzing intensity data because intensity will vary depending on the instrumentation and experimental setup whereas lifetime does not.
Utilizing fluorescence lifetime information appears as an attractive method to study the re-binding of small molecules such as CO to the heme. However, if the binding-unbinding process is too fast, individual states will not be well separated in a lifetime trajectory, and it will not be easy to obtain the lifetime information. In this chapter, our aim is to optimize the FRET efficiency in a labeled Mb by a proper choice of dye and of the labeling position. Then, we will have to show that the different Mb states can be identified reliably on the basis of their fluorescence lifetime and/or fluorescence intensity.
In other words, our aim is to prove that it is possible to distinguish FRET rates in Mb and MbCO, and to study the kinetics of rebinding of CO to Mb by means of fluorescence lifetime measurements, and It may also be possible by fluorescence intensity measurements.

4.2. Results

4.2.1 Labeling position and fluorescent dye selection

Selection of the proper dye is crucial. A range of available and photostable dyes with their fluorescent properties including wavelength of maximum emission, lifetime, quantum yield and calculated R_0 related to deoxy-Mb and MbCO are given in Table 4.1. R_0's have been calculated based on Eq (1.1) in Chapter 1 in which the donor is the fluorescent dye and the acceptor is the heme center of deoxy-Mb and MbCO. R_0 (in Å) is given by: [13]

$$R_0 = 0.2108 \left(\frac{\kappa^2 \phi_D}{n^4} \int \bar{F}_D(\lambda)\epsilon_A(\lambda)\,\lambda^4 d\lambda\right)^{\frac{1}{6}} \qquad 4.1$$

where ϕ_D is the fluorescence quantum yield of the donor in the absence of the acceptor, κ^2 is the dipole orientation factor and can vary between 0 and 4 (here we assume an isotropic angular distribution of the dye, thus the average orientational factor is $\kappa^2 = \frac{2}{3}$), n is the refractive index of the medium (here we assume a water medium thus the refractive index is $n = 1.33$ and more appropriate is to use 1.4; a mixture between buffer ($n = 1.33$) and protein $n = 1.5$), $\epsilon_A(\lambda)$ is the acceptor molar extinction coefficient ($M^{-1}cm^{-1}$). In this work, the acceptors are deoxy-Mb and MbCO

and their molar extinction coefficient values were extracted from ref. [7], and $\bar{F}_D$ is the donor emission spectrum normalized to an area of 1 ($\int_0^\infty F_D(\lambda)d\lambda = 1$). In this work, $\bar{F}_D$ is calculated based on the the donor emission spectra of the fluorescent dyes (Table 4.1) obtained from ref. [14,15]
The fluorescence emission spectra corresponding to these dyes are shown in Figure 4.2.

Table 4.1 *Photostable dyes with their fluorescent properties including wavelength of maximum emission (λ_{em}), quantum yield (ϕ_D), lifetime (τ),[14,15] and calculated R_0 for deoxy-Mb and MbCO.*

Dye[a]	λ_{em}	ϕ_D	τ	R^b_0	R^b_0
				MbCO	**deoxy-Mb**
ATTO Rho14	646 nm	80%	3.7 ns	2.72 nm	3.73 nm
ATTO 633	651 nm	64%	3.4 ns	2.53 nm	3.56 nm
ATTO 647	667 nm	20%	2.4 ns	1.98 nm	2.89 nm
ATTO 643	**664 nm**	**65%**	**3.5 ns**	**2.46 nm**	**3.54 nm**
ATTO 655	680 nm	30%	1.8 ns	2.08 nm	3.07 nm
ATTO Oxa12	681 nm	30%	1.8 ns	2.09 nm	3.07 nm
ATTO 680	698 nm	30%	1.7 ns	2.02 nm	3.04 nm
ATTO 700	716 nm	25%	1.6 ns	1.95 nm	2.93 nm
ATTO 725	751 nm	10%	0.5 ns	1.66 nm	2.53 nm
ATTO 740	**763 nm**	**10%**	**0.6 ns**	**1.66 nm**	**2.54 nm**
Cy7	**773 nm**	**30%**	**0.5 ns**	**2.00 nm**	**2.99 nm**

[a] All fluorescent properties of the dyes reported based on the manufacturer's data [14,15]
[b] The R_0 values for the deoxy-Mb and MbCO were calculated based on equation 4.1, the room temperature spectra of Mb, and the assumptions mentioned in section 4.2.1.

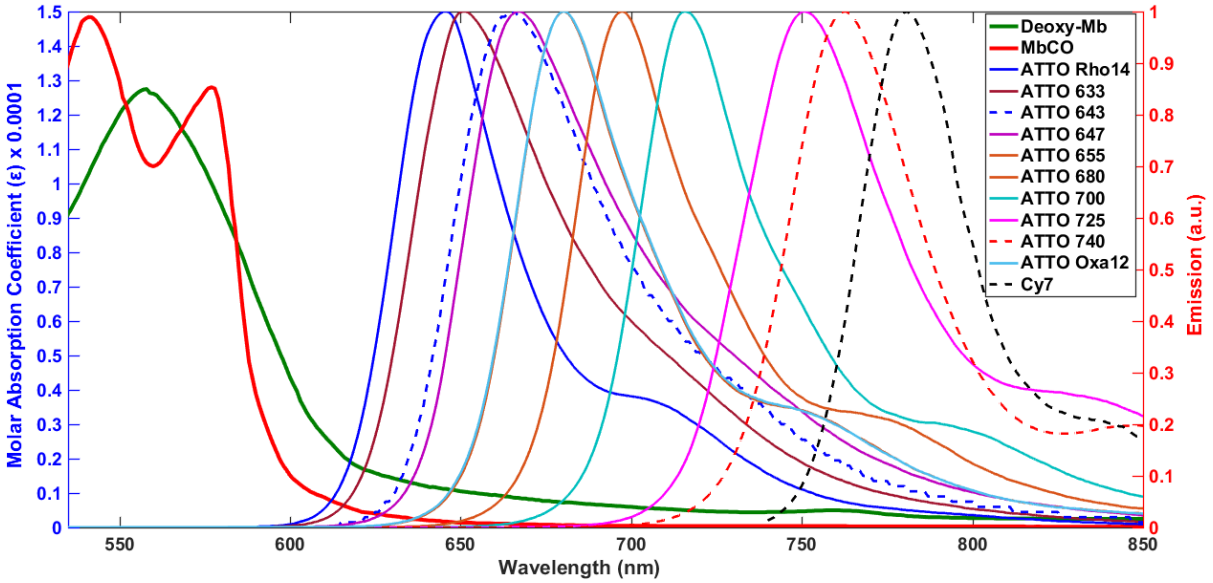

Figure 4.2 *The absorption spectra of deoxy-Mb (solid green) and MbCO (solid red) (left axis),* [7] *and fluorescence emission spectra of various dyes listed in table 1 as donors in phosphate buffer, pH=7 (right axis).* [14,15] *ATTO 643 (dashed blue), Cy7 (dashed black), and ATTO 740 (dashed red) are the fluorescent dyes selected as donors for our FRET experiments.*

While there are many fluorophores available for protein labeling, few are suitable for estimating the quantum yield of MbCO bond breaking by NIR excitation.
We have selected ATTO 643 dye as the donor in this FRET study of Mb. Atto643 dye has a maximum absorption at 643 nm (Figure 4.2) and it emits with a maximum intensity at 664 nm with a quantum yield of 65% (Table 4.1). It is a standard dye; it is easily available and it is a safe dye with neutral charge when attached to the protein. It might minimize specific dye-protein interaction. It has also a long fluorescence lifetime (compare to NIR dyes).
To study the quantum efficiency of breaking the Mb-CO bond with light in the NIR area, a dye is needed that absorbs and emits in this region of the spectum. For this purpose, we have selected Cy7 and ATTO 740 as photostable dyes which are excited at the wavelengths of 750 nm and 743 nm respectively, and which are far enough from the Q-bands of Mb-CO (500-700 nm) that their fluorescence cannot excite the Q-bands. Therefore, when attached to the protein, these dyes cannot excite the π electrons of the heme, but they only excite transitions of the iron itself. The wavelengths of maximum emission for Cy7 and ATTO 740 are 773 nm and 763 nm respectively, in a region where the absorbances of deoxy-Mb and MbCO are very different.
The main parameter that influences the FRET efficiency is the distance between donor and acceptor (see Chapter 1). Different positions of the dye on the protein provide different distances between donor and acceptor. Apart from the N-terminus, proper labeling positions can be achieved by site-directed mutagenis (SDM).
Among the 20 amino acids, cysteine is uniquely reactive and engineered cysteine residues are common targets for specific labeling of proteins. The thiol group of cysteine reacts efficiently with the maleimide functional group of a fluorescent dye via the Munich reaction. Mb has no cysteines but cysteines can be engineered in Mb by SDM.

In this study, we used the Mb variant S3C from sperm whale (*Physeter macrocephalus*), in which serine 3 has been replaced by cysteine. The plasmid for this mutant was kindly provided by Prof. G. Ulrich Nienhaus (Karlsruhe Institute of Technology). The mutant protein was expressed in *Escherichia coli*.
Although labeling at a position closer to the heme provides higher FRET efficiency, the local steric and electrostatic characteristics around an engineered cysteine and its accessibility are also important. Moreover, keeping the labeling position away from the heme avoids disturbing the protein reaction center. The mutation at serine 3 (Figure 4.3) satisfies these considerations and provides a distance of approximately 27.4 Å from the heme center.

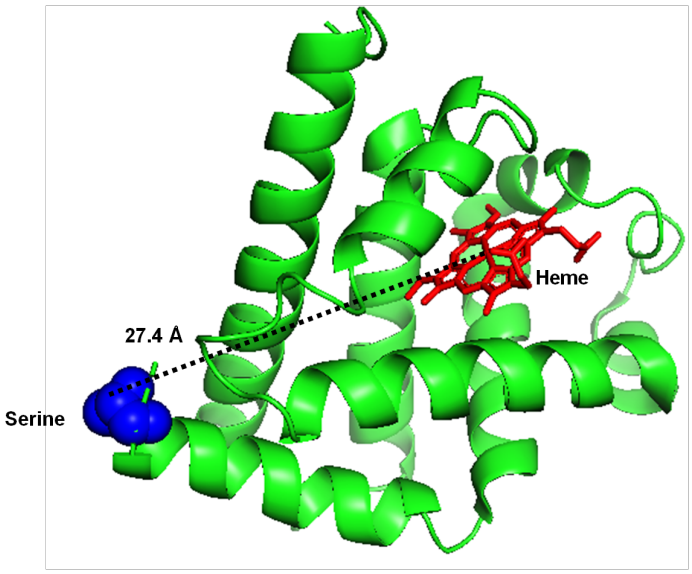

Figure 4.3 *Scheme of native sperm whale met-Mb from the Protein Data Bank (PDB: 1VXA5) indicating the heme (red), and amino acid serine 3 (site of mutation for labeling) is shown as spheres (blue). Estimation of the distance between dye and heme based on PyMOL* [16] *distance calculations. The distance between serine 3 and the center of the heme was calculated to be 27.4 Å.*

An alternative, non-mutagenic labelling method is targeting the N-terminus of Mb. This allows for more free space of the dye and diminishes the electrostatic interaction with the protein. The general systematic strategy in this case is to react the free amine of the amino acid in the protein with the reactive functional group (carboxylic or N-hydroxy succinimide (NHS)) of the modified dye. By controlling pH, and the concentrations of dye and protein, we could achieve specific N-terminal labeling with high efficiency. This labeling strategy provides an easy way to install a label on the N-terminal glycine 1 in commercially available horse heart Mb. Figure 4.4 shows horse heart met-Mb which is slightly different from sperm whale met-Mb particularly in the N-terminus. The distance between the N-terminus and the heme in horse heart met-Mb is slightly shorter (24.2 Å, Figure 4.4) than between heme and serine 3 (27.4 Å). Labeling with cysteine, however, is site specific and clean.

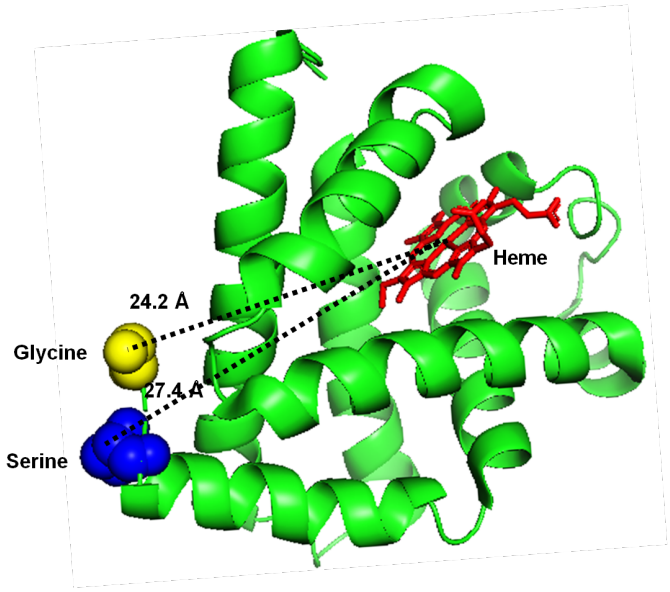

Figure 4.4 *Scheme of horse heart met-Mb from the Protein Data Bank (PDB: 1WLA) indicating the heme (red), and the N-terminal glycine 1 (site of labeling) is shown as spheres (yellow). Estimation of the distance between dye and heme based on PyMOL* [16] *distance calculations. The distance was calculated based on the distance from glycine 1 to the center of heme (24.2 Å) and compared to the distance of the heme center to the serine 3 (blue) (27.4 Å).*

4.2.2 Preparation of labeled Mb variants

Met-Mb was labeled with the selected dyes of the previous section (ATTO 643, Cy7, and ATTO 740). Labeling of met-Mb was performed using two approaches specifically at position cysteine 3 (mutagenesis serine 3) and by N-terminal labeling. Then, as discussed in Chapter 3 (section 3.2.1), labeled met-Mb was converted to dye-labeled deoxy-Mb and to MbCO.

4.2.3 Materials and equipment

All chemicals were commercial products with the best quality available and, unless indicated otherwise, they were used without further purification. All solvents were purchased from Sigma-Aldrich with high purity and directly used for the experiments except DMF, which was dehydrated with Molecular Sieves (Sigma-Aldrich) before use. *Physeter macrocephalus* (sperm whale) Mb variant S3C was expressed in *Escherichia coli* and purified. The plasmid for this mutant was kindly provided by Prof. G. Ulrich Nienhaus (Karlsruhe Institute of Technology). Horse heart Mb was purchased from Sigma-Aldrich with a molecular weight of 17.7 kD.
UV-Vis absorption spectra were obtained using a droplet spectrophotometer with a light path of 1 mm and a UV-Vis spectrophotometer (Cary 50, Variant Inc., Agilent Technology, USA) with a light path of 10 mm.

4.2.4 Labeling and characterization of met-Mb

Labeling was performed as recommended by the research group of Prof. Don C. Lamb at the Ludwig-Maximilians-Universität, München (LUM). Mutated sperm whale met-Mb

variant S3C was labeled using commercially available ATTO 643 maleimide (ATTO-TEC GmbH, Siegen, Germany) and Cy7 maleimide, which reacts with a high yield to the thiol group of cysteine. Labeling was performed in two steps: First, unreactive disulfide bonds of mutated Mb were reduced with a ten-fold molar excess per cysteine of DTT (1,4-Dithiothreitol, Sigma-Aldrich) in potassium phosphate buffer (100 mM) at pH 7.2. To increase the efficiency of reduction, in addition, a 5-fold molar excess of TCEP (Tris(2-carboxyethyl)phosphine) per cysteine was added to the protein solution, and then the solution was flushed with Argon gas (Ar) in a desiccator. The mixture was kept for 20–30 minutes at room temperature. Removal of DTT before dye conjugation was done by four runs in a Vivaspin centrifugal concentrator (Sartorius VS0111, MWCO 10000, 500 uL) for 10 minutes with an acceleration of 10,000 g at 10 °C. Secondly, the mutated met-Mb in potassium phosphate buffer (100 mM) was allowed to react with a 3-3.5 molar excess of label dissolved in fresh DMSO solvent (Sigma-Aldrich), and incubated overnight in the dark at room temperature. To remove the unbound dye (Figure 4.5), the solution was washed repeatedly by centrifugation to a final dilution of 10^{-6}. Separation of the labeled protein from free dye was established firstly by using a Corning® Spin-X® UF 20 concentrator (polyethersulfone membrane (PES), Molecular weight cut-off (MWCO) 10 k, 20 ml) twice for 10 mins at 10 °C with acceleration 1,200 g and then further purification was done with an ultrafiltration centrifugal micro-concentrator (Sartorius VS0111, MWCO 10000, 500 uL) for 10 min at 10 °C with an acceleration of 10,000 g to a final dilution of 10^{-6}. Washing was performed for each run at 10 °C to prevent denaturation, the concentrated protein was diluted with phosphate buffer (pH=7.2) and subjected to centrifugation cycles. For long-term storage, labeled Mb was divided into aliquots and frozen at -80 °C.

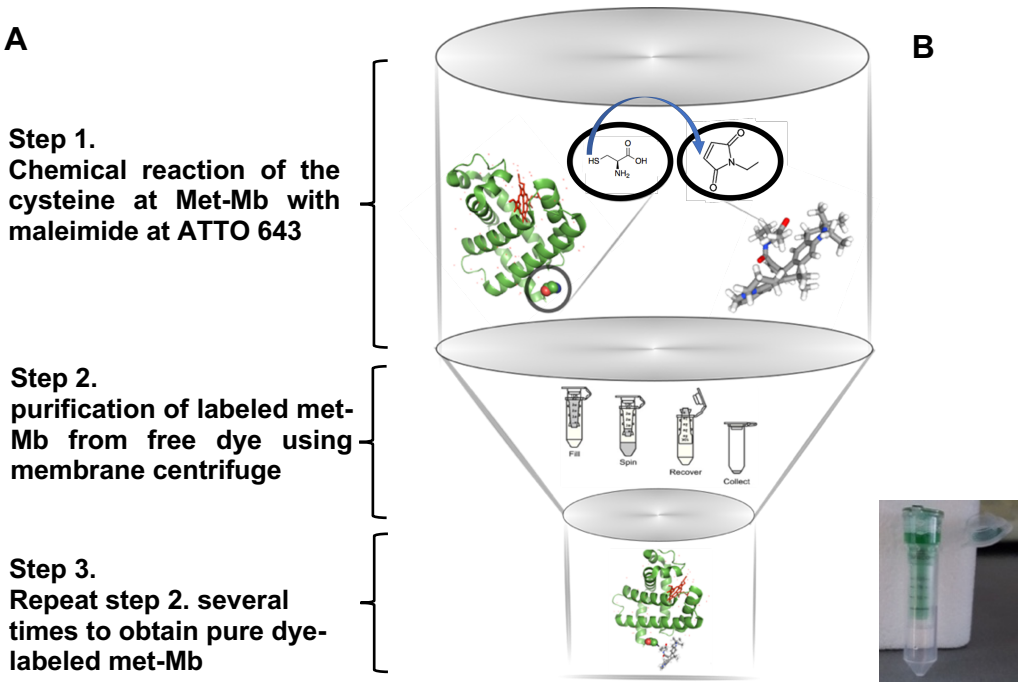

Figure 4.5 *(A) A schematic for labeling of cysteine-mutated met-Mb with ATTO 643 maleimide and purification of labeled met-Mb from the free dye using membrane centrifugation. (B) membrane centrifuge MWCO of 10 k used for separation of free dye after labeling of met-Mb.*

N-terminal labeling was performed by the same protocol as for the cysteine 3 (mutagenesis serine 3) Mb except without the addition of DTT and TCEP. The N-terminus labeling protocol as recommended by Jena Bioscience GmbH was followed. [17] According to this method, horse heart met-Mb (Sigma-Aldrich) was N-terminally labeled with ATTO 740 NHS (N-Hydroxy succinimide) (ATTO-TEC GmbH, Siegen, Germany), which reacts with the NH_2 group of the N-terminus in PBS buffer (Sigma-Aldrich) at pH=7.2. However, before this reaction, the N-terminus was activated by adding sodium bicarbonate (1 M) (Sigma-Aldrich) to the protein solution to reach a final concentration of 100 mM and the mixture was vortexed shortly. Then, ATTO 740 label dissolved in dehydrated DMF solvent (Sigma Aldrich) was reacted with met-Mb in PBS (10 mM) with a dye to protein ratio of 3-3.5 for 2-3 hours at room temperature in the dark. The free unbound dye was removed through several centrifugation steps by the Vivaspin centrifugal concentrator (Sartorius VS0111, MWCO 10000, 500 uL) for 10 minutes at 10 °C to reach a final dilution of 10^{-6}. The purified labeled Mb was stored in aliquots at -80 °C.
The degree of labeling (DOL) specifies the average number of fluorophore molecules per molecule of conjugate. The DOL was determined for the cysteine 3 met-Mb from UV-Vis absorption spectra (Figures 4.6, and 4.7) obtained from a droplet spectrophotometer with a light path of 1 mm. For N-terminally labeled met-Mb the absorption spectra (Figure 4.8) were measured on a UV-Vis spectrophotometer (Cary 50, Variant Inc., Agilent Technology, USA) with light path of 10 mm.

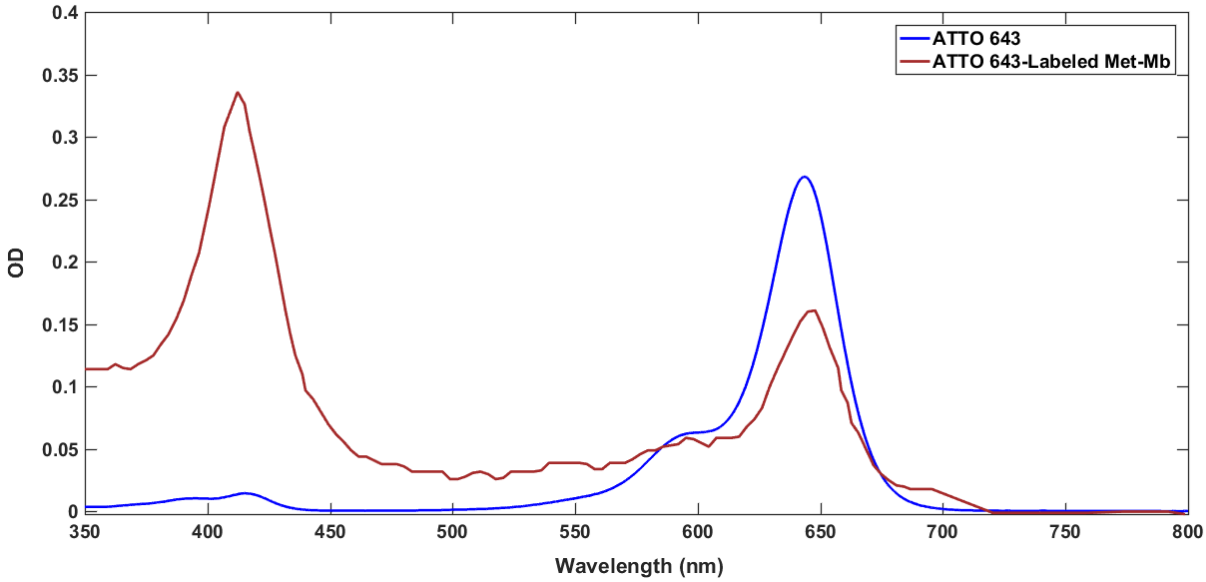

Figure 4.6 *Absorption spectrum of free ATTO 643 maleimide dye (blue) and ATTO 643-labeled mutated met-Mb (red) in potassium phosphate buffer (100 mM) at pH 7.2. Absorption at 409 nm arises from the Soret band of met-Mb, while the peak at 646 nm is due to the ATTO 643 dye.*

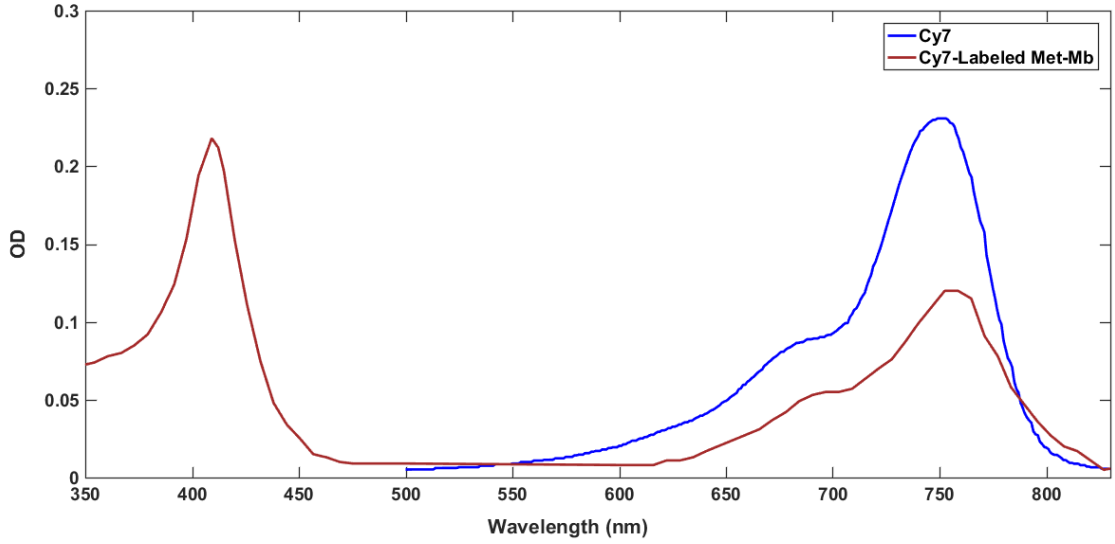

Figure 4.7 *Absorption spectrum of free Cy7 maleimide dye (blue) and Cy7 labeled-mutated met-Mb (red) in potassium phosphate buffer (100 mM). Absorption at 409 nm arises from the Soret band of met-Mb, while the peak at 751 nm is due to the labeled Cy7 dye.*

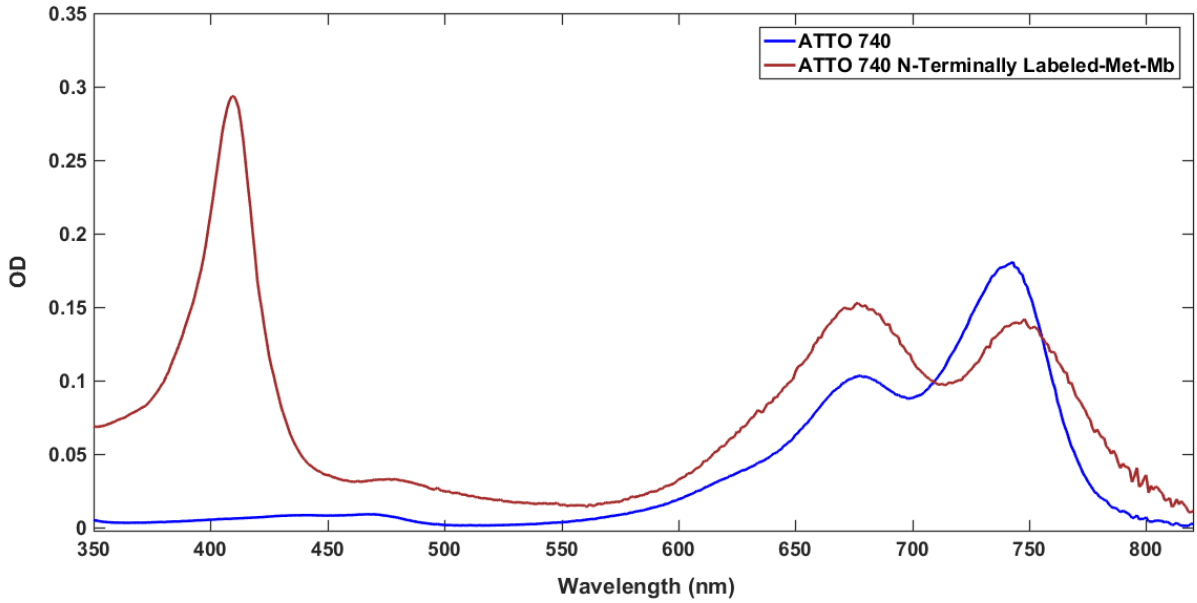

Figure 4.8 *Absorption spectrum of free ATTO 740 NHS dye (blue) and N-terminally labeled-met-Mb (brown) in PBS buffer (10 mM) at pH 7.2. Absorption at 409 nm arises from the Soret band of met-Mb while the peaks at 680 nm and 740 nm are due to the labeled ATTO 740 dye.*

The concentration of bound dye and labeled protein are given by: $c = A_{max} / (\varepsilon_{max} \times d)$, where ε_{max} is the extinction coefficient of the dye or protein at the absorption maximum and d is the path length of light in solution. The maximum absorption (A_{max}) of met-Mb, ATTO 643, Cy7, and ATTO 740 are at the wavelengths of 409 nm, 646 nm, 751 nm, and 740 nm (λ_{max}) respectively. The CF (Correction Factor), which is the ratio of $\varepsilon_{280} / \varepsilon_{max}$ for DOL calculation, have been reported (Table 4.2).

The DOL is calculated according to following formula: [17]

$$DOL = (A_{max} / \varepsilon_{max}) / (A_{protein} / \varepsilon_{protein}) \quad 4.2$$

$$DOL = (A_{max} \times \varepsilon_{280}) / ((A_{280} - A_{max} \times CF_{280}) \times \varepsilon_{max}), \quad 4.3$$

where A_{280} is the absorbance of the conjugate solution measured at 280 nm, A_{max} is the absorbance of the conjugate solution measured at λ_{exc}, the λ_{exc}, ε_{max}, and CF_{280} are intrinsic properties of the fluorescent dye, and ε_{280}, M_W are intrinsic properties of the used protein.

Table 4.2 *Spectral information of Met-Mb, ATTO 643, Cy7, and ATTO 740 in PBS at pH= 7.4 at 22 ºC.*

Sample	**λ_{max} (nm)**	**Maximum molar extinction coefficient (ε_{max})[a] M^{-1} cm^{-1}**	**Correction Factor (CF_{280})[a] (ε_{280} / ε_{max})**
Met-Mb	280	43900	-
Met-Mb	409	188000	-
ATTO 643	646	150000	0.04
Cy7	751	199000	0.029
ATTO 740	740	120000	0.07

[a] *as specified by the manufacturer*

The ratio of bound dye and the amount of reacted protein yields the DOL by eliminating the absorbance of the dye coupled to the protein. Regarding calculation of the protein concentration, there are two options: using the absorption of conjugate met-Mb at the Soret-band (409 nm), or the absorption of conjugate met-Mb at 280 nm. The two possibilities have been tried to calculate the DOL for met-Mb labeled at the N-terminus with ATTO 740. The DOL calculated on the basis of formula (Eq. 4.3) was 69.1% and the calculated DOL based on the absorption of conjugate protein at Soret-band (409 nm) was 73.1% (Eq. 4.2). Calculation by the first method for ATTO 643 and Cy7 labeled met-Mb (Table 1), yielded DOL's of 61.6%, and 51.7%, respectively.

4.2.5 Preparation of ATTO 643-, Cy7-, and ATTO 740 -labeled deoxy-Mb and MbCO

We labeled S3C sperm whale met-Mb with ATTO 643 and Cy7. We labeled horse heart met-Mb with ATTO740. From those, we obtained labeled deoxy-Mb and MbCO as described in Chapter 3, section 3.2.1. Figure 4.9 shows one example, the absorption spectrum of ATTO 643-labeled S3C MbCO in phosphate buffer (pH=7.2).

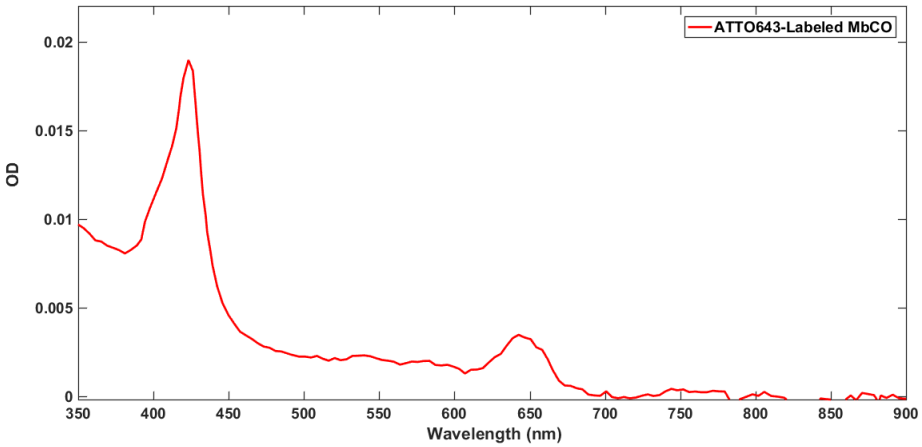

Figure 4.9 *Absorption spectrum of ATTO 643-labeled S3C MbCO in potassium phosphate buffer (100 mM) at pH 7.2. The band at 422 nm is the Soret band of MbCO, while the peak at 646 nm is due to the ATTO 643 dye label.*

4.2.6 Ensemble fluorescence lifetime measurements of ATTO 643-, Cy7-, and ATTO 740-labeled Mb

Two setups for fluorescence lifetime measurement have been used. One experiment has been done in Munich at the laboratory of Prof. Don C. Lamb in LMU and the other setup was a homemade microscope in Leiden University.
The setup in Munich for fluorescence lifetimes was an Edinburgh FLS1000 (Edinburg Instruments, Livingston, United Kingdom) fluorescence lifetime spectrometer (Figure 4.10). Decay measurements were performed using time-correlated single-photon counting (TCSPC). The dyes were excited using 640 nm and 730 nm lasers for ATTO 643 and Cy7, respectively.

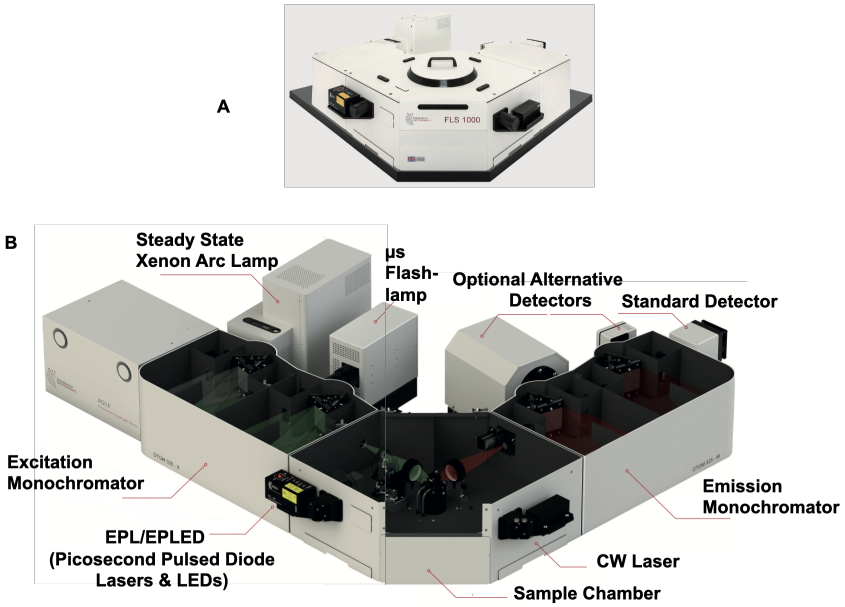

Figure 4.10 *(A) Schematic of the fluorescence lifetime spectrometer FLS 1000 at the LMU, (B) Details of the FLS 1000 setup for lifetime measurement of ATTO 643, Cy7, and labeled protein [after [18]].*

The setup in Leiden university was a homemade microscope in which ATTO 740 is excited with a pulsed laser at 636 nm with a pulse repetition rate of 26 MHz, which was the red-most laser available but was not optimal for ATTO740 excitation. The schematic illustration of the setup is shown in Figure 4.12. The collected photons were quantified with time-correlated single-photon counting (TCSPC) and converted by the SymphoTime software to lifetime data. Figure 4.13 shows the designed mini-cuvette with an inlet and outlet for bubbling gas inside the solution on top of the microscope for the preparation of deoxy-Mb and MbCO from met-Mb state as described in Chapter 3, section 3.2.1.

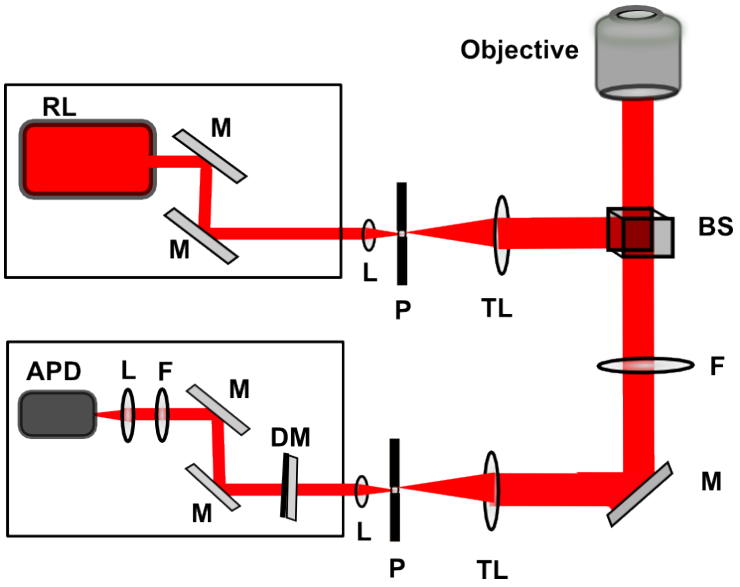

Figure 4.12. *A schematic of the home-made confocal microscope setup of Leiden University used for the lifetime measurement of ATTO 740 and ATTO 740-labeled protein. RL=Red Laser, M=Mirror, L=Lens, P=Pinhole, TL=Telescope (Beam Expander), BS=Beam splitter, F=Filter, DM=Dichroic Mirror, APD=Avalanche Photodiode Detector.*

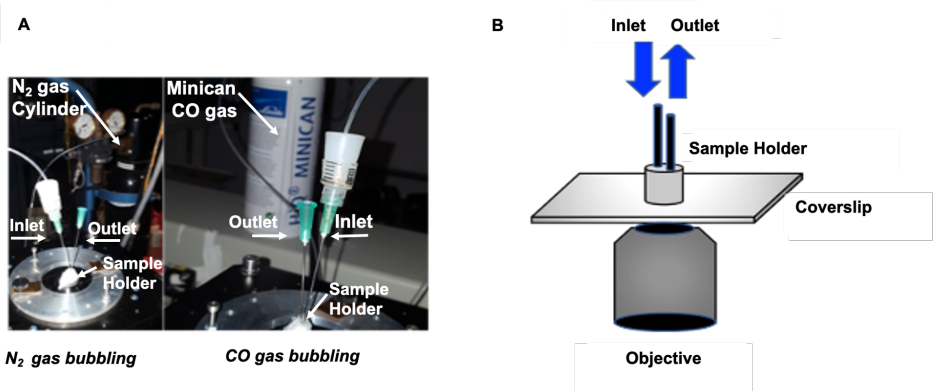

Figure 4.13 *(A) A picture of the microscope used for lifetime measurement showing the sample holder on top of microscope with inlet and outlet paths for N_2 or CO gas bubbling. Lifetime measurements were performed in the solution while focusing the laser beam 5-10 microns above the glass. (B) The designed sample holder (volume 10 µL) with inlet and outlet pathways for gas bubbling to preparate deoxy-Mb and MbCO from met-Mb on the microscope.*

4.2.7 Comparison of ensemble fluorescence lifetime measurement of ATTO 643-, Cy7-, and ATTO 740-labeled deoxy-Mb, MbCO, and met-Mb

First, we measured the fluorescence lifetimes of ATTO 643 (170 nM), Cy7 (177 nM) dyes alone and of ATTO 643-(170 nM), and Cy7-labeled (177 nM) deoxy-Mb, MbCO, and met-Mb in potassium phosphate buffer; pH=7.2 using the Edinburgh FLS1000 instrument for 5 minutes and exciting with a pulsed laser at 640 nm with a pulse rate of 21 MHz. The photons collected using TCSPC were converted by the SymphoTime software to lifetime data. Figures 4.10, and 4.11 and Table 4.3 show the results of fluorescence lifetime measurements for ATTO 643 and Cy7 dyes and ATTO 643-, and Cy7-labeled deoxy-Mb, MbCO, and met-Mb.

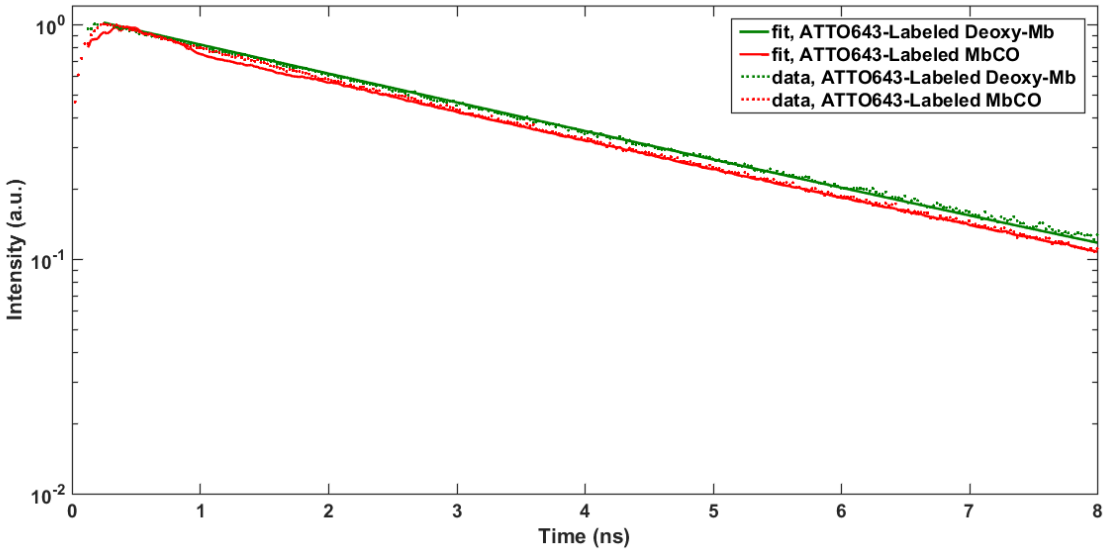

Figure 4.10 *Fluorescence decays of ATTO 643-labeled deoxy-Mb (green), and MbCO (red) in potassium phosphate buffer (100 mM) at pH 7.2. Experimental data (dotted lines) and single-exponential fits (solid lines).*

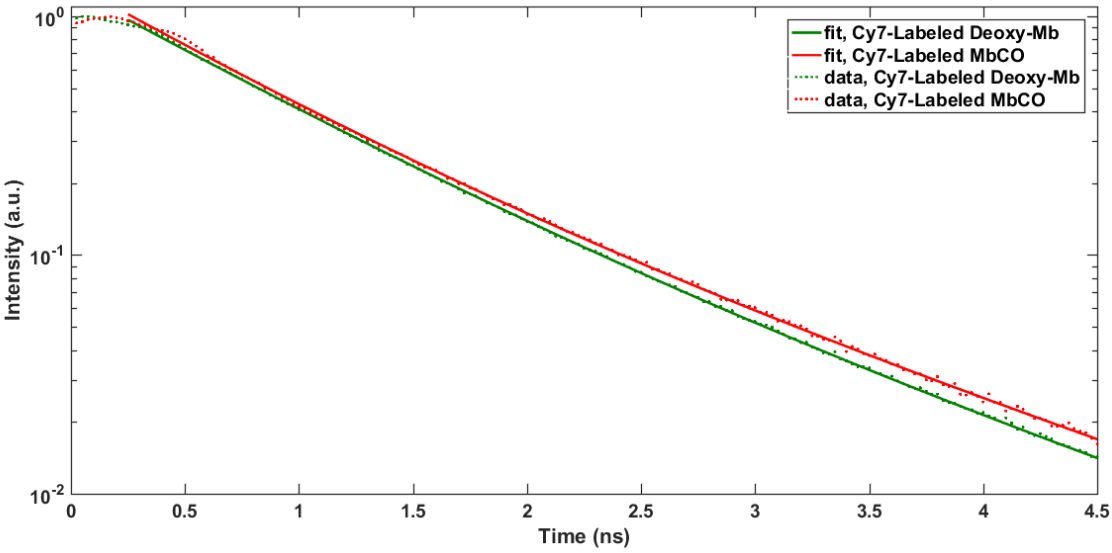

Figure 4.11 *Fluorescence decays of Cy7-labeled deoxy-Mb (green) and MbCO (red) in potassium phosphate buffer (100 mM) at pH 7.2. Experimental data (dotted lines) and bi-exponential fits (solid lines).*

Table 4.3 *Comparison of the fluorescence lifetimes of ATTO 643 dye (170 nM) and Cy7 (177 nM) and ATTO 643, and Cy7-labeled deoxy-Mb, MbCO, and met-Mb in potassium phosphate buffer (100 mM), pH=7.2, at room temperature. Excitation was performed using a pulsed laser at 640 nm and 21 MHz repetition rate.*

Sample	**Experimental Lifetime (ns)**
ATTO 643 dye	3.6[a]
ATTO 643 -deoxy-Mb	3.54
ATTO 643 -MbCO	3.30
ATTO 643 -met-Mb	2.75
Cy7 dye	0.45 [b]
CY7-deoxy-Mb	0.84
CY7-MbCO	0.81
CY7 -met-Mb	0.70

[a] *lifetime specified by the manufacturer as 3.5 ns in PBS buffer, pH =7.4 and 22 º C*
[b] *lifetime as specified in literature is 0.43 ns* [19]

As can be seen, there is a quenching effect in the ATTO 643 and Cy7-labeled met-Mb form compared to ATTO 643 and Cy7-labeled deoxy-Mb forms. In contrast, there is almost no difference between the lifetimes of the ATTO 643, and Cy7-labeled deoxy-Mb and MbCO forms of Mb. For the Cy7 label, the measured lifetime of the free dye is significantly shorter (0.45 ns) than of the attached dye, which may be because of the environmental sensitivity of Cy7 fluorophore, for example, by limiting dye distortions and conformational fluctuations. It should be noted that in fitting the data, the decays were considered to be mono-exponential.
Secondly, we measured the fluorescence lifetimes of free ATTO 740, and ATTO 740-labeled deoxy-Mb, MbCO, and met-Mb using our homemade setup in Leiden University. The sample was in PBS buffer, pH=7.2, in a cuvette and was excited with a pulsed laser at 636 nm with a repetition rate of 26 MHz for 4 minutes. The collected photons were quantified using TCSPC and converted by the SymphoTime software to lifetime data. Figures 4.14, 4.15, 4.16 and Table 4.5 show the results of the fluorescence lifetime measurements.

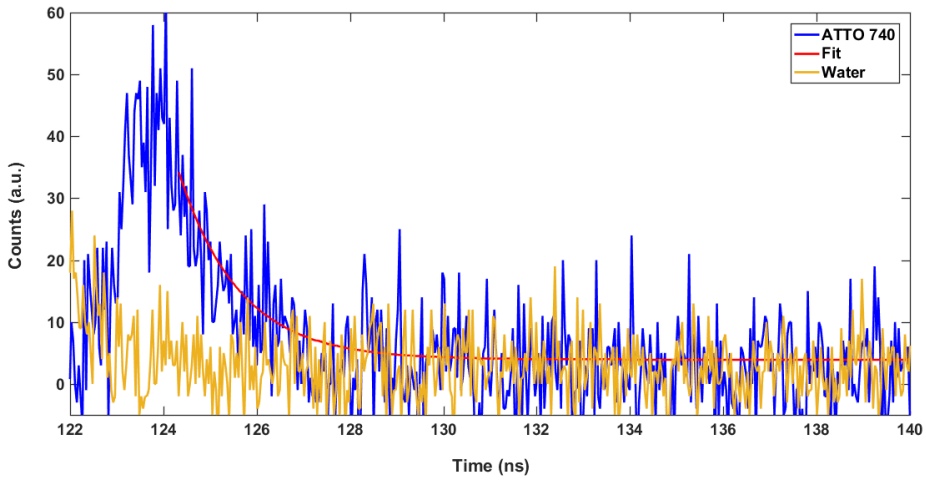

Figure 4.14 *Fluorescence decays of free ATTO 740 dye (blue), the fit (red), and water (yellow).*

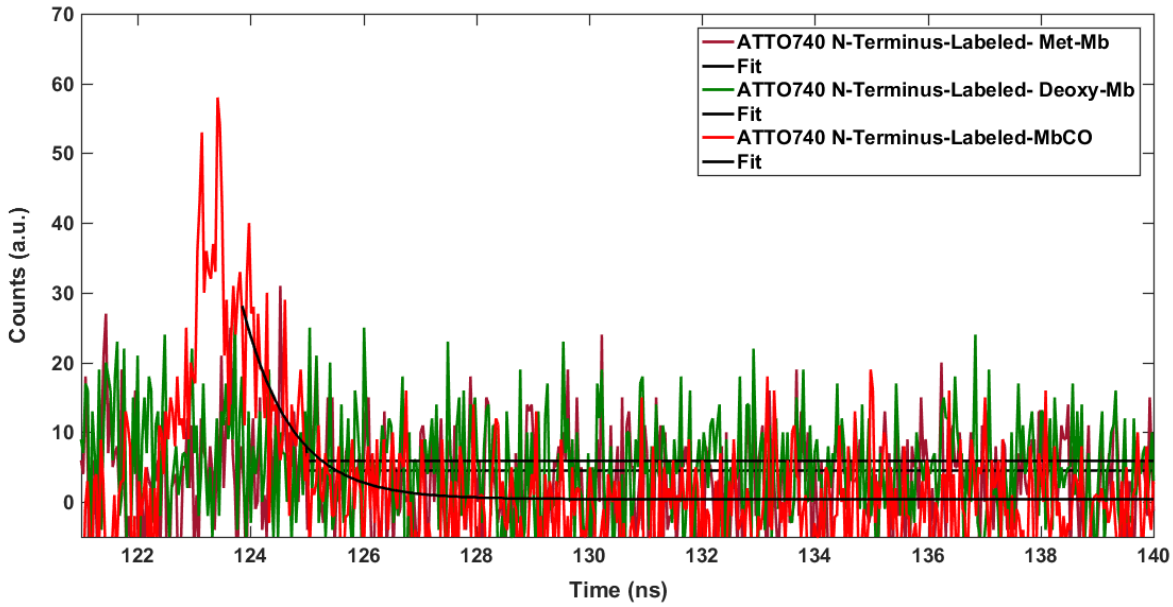

Figure 4.15 *Fluorescence decays of ATTO 740 -labeled met-Mb (purple), ATTO 740 -labeled deoxy-Mb (green), ATTO 740 -labeled MbCO (red), and the respective fits (black).*

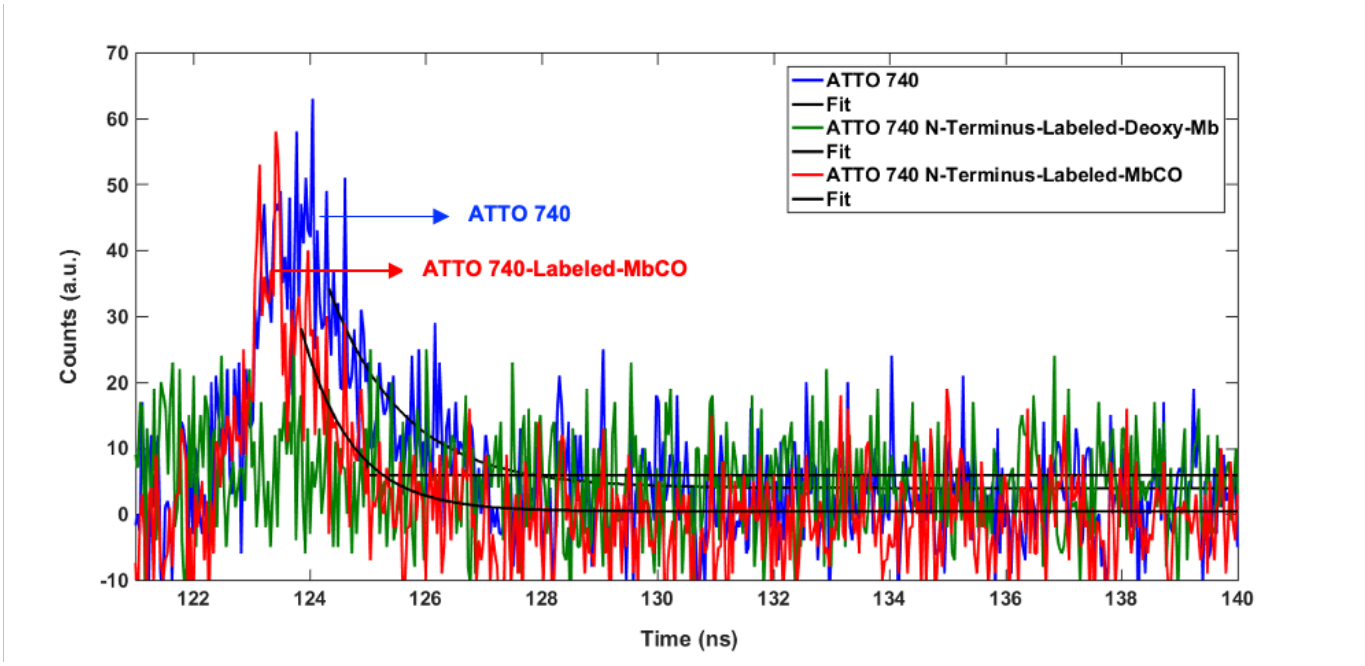

Figure 4.16 *Comparison of the fluorescence decays of free ATTO 740 (blue), ATTO 740 -labeled-deoxy-Mb (green), ATTO 740 -labeled-MbCO (red), and the respective fits (black).*

Table 4.5 *Fluorescence lifetimes of ATTO 740 and ATTO 740-labeled deoxy-Mb, MbCO, and met-Mb.*

Sample	Experimental Lifetime (ns)
ATTO 740 dye	1.2 [a]
ATTO740 labeled-deoxy-Mb	N.A.
ATTO740 labeled-MbCO	0.87
ATTO740 labeled-met-Mb	N.A.

[a] *lifetime specified by the manufacturer as 0.65 ns in PBS buffer, pH =7.4 and 22 º C*

Figure 4.14 demonstrates the decay of free ATTO 740 dye (177 μM) compared to a blank sample (water). The measured lifetime was 1.2 ns. The fluorescence trace of a solution of met-Mb N-terminally labeled with ATTO 740 (234 μM, containing 177 μM dye based on a calculated 75% DOL) was measured for 4 minutes before and after reduction with sodium dithionite under oxygen-free atmosphere and N_2 bubbling to produce the deoxy form. Finally, the sample was bubbled with CO gas for 10 minutes and the fluorescence decay was followed for 4 minutes under the same conditions as for the dye labeled-deoxy and met-Mb samples. Figure 4.15 shows the fluorescence decays of ATTO 740 -labeled-met-Mb (intensity close to background)), ATTO 740 -labeled deoxy-Mb (intensity close to background)), and ATTO 740-labeled MbCO (Intensity of 40 counts, lifetime 0.87 ns). In Figure 4.16, the fluorescence decay of free ATTO 740 (intensity of 50 counts, lifetime 1.2 ns) has been compared to the ATTO 740 N-terminus-labeled-deoxy-Mb and ATTO 740 -labeled-MbCO (red), and fit (black). The measured lifetimes are collected in Table 4.5.
For the ATTO 740-labeled met-Mb and deoxy-Mb forms, the fluorescence intensity is low because of quenching by the absorption bands of met-Mb and deoxy-Mb, whereas a higher intensity is observed for ATTO 740 labeled-MbCO, which has much less absorption in the near infra-red region.
Because of low intensity, low signal-to-noise ratio, and interference with the IRF (tau~ 0.6 ns), the data collected in this experiment can be interpreted based on only the difference in intensities and not on measured lifetime data.

4.3 Discussion

4.3.1 Fluorescent labelling and preparation of the different states of Mb

In summary, the purification and dye-labeling of Mb yielded a degree of labeling of 50-65% for sperm whale Mb variants and 65-75% for N-terminus labeling of horse heart Mb (Figures 4.6-4.8).
ATTO643-, Cy7-, and ATTO740-deoxy-Mb, and -MbCO (Figures 4.9) were prepared with the same protocol as used for the preparation of unlabeled deoxy-Mb and MbCO and the preparations exhibited the expected absorption spectrum containing the respective Soret-band, Q-bands and NIR bands.

4.3.2 Comparison of calculated Förster resonance energy transfer parameters and experimental lifetime

In this section, we calculate the Förster resonance energy transfer parameters such as Förster radius (R_0), energy transfer rate (k_{ET}), and energy transfer efficiency (E)

for ATTO643-, Cy7-, and ATTO740-deoxy-Mb, and MbCO and then compare the calculated results with the experimental data and the lifetimes of the corresponding free dyes.

4.3.3 Förster resonance energy transfer radius (R_0)

The Förster resonance energy transfer (FRET) efficiency and R_0 have been calculated using equation (1.1) in chapter 1.
The Förster radii of deoxy-Mb and MbCO labeled with ATTO 643 and Cy7 were calculated in MatLab (The MathWorks, Inc., Natick, Massachusetts, United States.) using the spectra published by Bowen [7]. For all calculations, κ^2 was assumed to be 2/3 and the refractive index was set at n=1.33. The results are given in Table 4.1.

4.3.4 Förster Resonance Energy Transfer Rate (k_{ET}) and Energy Transfer Efficiency (E)

The rate of energy transfer (k_{ET}) has been calculated with the following equation:

$$k_{ET} = \left(\frac{R_0}{r}\right)^6 \left(\frac{1}{\tau_D}\right) \qquad 4.4$$

To estimate the rates of energy transfer in dye-labeled Mb, the distance r between heme and dye was estimated based on two hypotheses. Hypothesis A is that the distance between dye and heme center is maximum (Figure 4.17A) and r is the distance of the heme center to the attachment position of the dye to the protein, including the full extended linker length ($r = r_P + r_{Linker}$). The other hypothesis, B, is that the two dipole moments are at the minimum distance (Figure 4.17B) and r is equal to the distance from the heme center to the attachment position of the dye to the protein, subtracting the linker length ($r = |r_P - r_{Linker}|$). Other possible positions will lie between these two above-mentioned extreme hypotheses. For example, by ignoring the linker length of dye r is equal to r_P (Figure 4.17C). It should be noted that the hypothesis of ($r = |r_P - r_{Linker}|$) in the reality is not true and can be ignored. It is depicted for comparison with other two possible hypothesis about r.

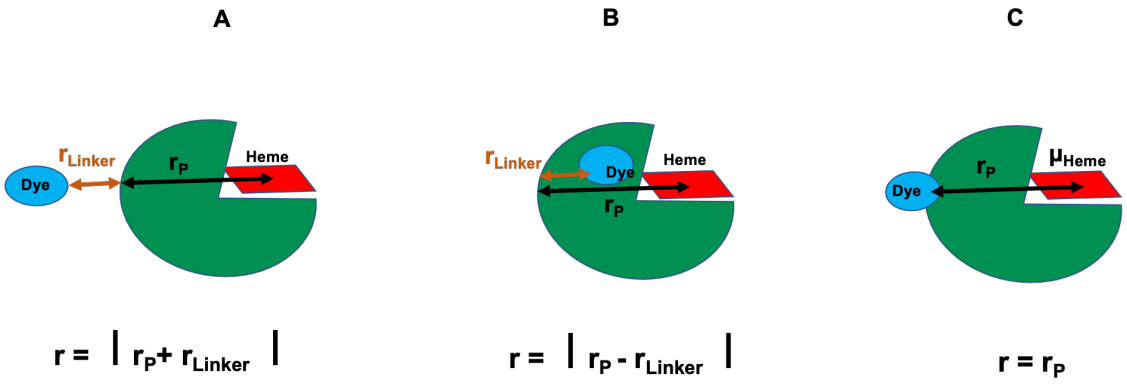

Figure 4.17 *Illustrative schema for r assumption in which r_P is the distance of heme center to the attachment position of dye to the protein and r_{Linker} is the linker length that connects the dye to the protein: (A) The dye is at the maximum distance to the center of heme ($r = |r_P + r_{Linker}|$), (B) The dye is at the minimum distance to the center of heme ($r = |r_P - r_{Linker}|$), (C) Ignoring the linker length of dye and r is equal to r_P.*

The distance between serine 3 and the center of the heme (r_P) is 27.4 Å (Figure 4.18A) in the crystal structure of sperm whale Mb (PDB: 1VXA) and the linker lengths to the core of the dye (r_{Linker}) are 11.3 Å (Figure 4.18B) and 15.7 Å (Figure 4.18C) for ATTO 643 and Cy7, respectively. All distance measurements were performed in PyMol. For the calculation of k_{ET} and E, we assume maximum distance between dye and the center of the heme (Figure 4.17A, r = | r_P + r_{Linker} |) which is estimated to be 38.7 Å and 43.1 Å for ATTO 643 and Cy7-labeled sperm whale Mb respectively (Figure 4.18).

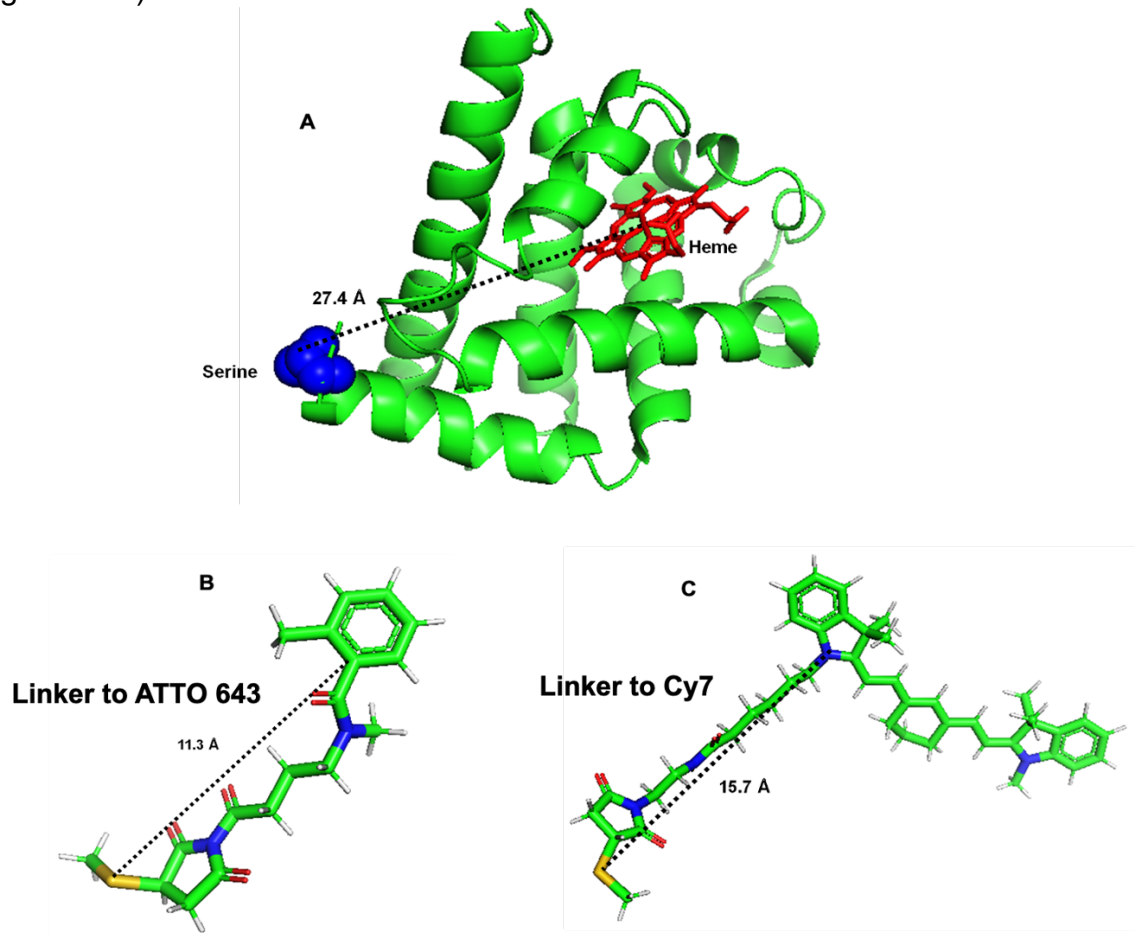

Figure 4.18 *Distance between dye and heme based on PyMOL distance calculations. The distance was calculated as the sum of (A) the distance from attachment position of dye on the serine 3 to the center of the heme (27.4 Å) in native sperm whale Mb (PDB: 1VXA) plus (B) the linker length to the ATTO 643 dye (11.3 Å), or (C) the linker length to the Cy7 dye (15.7 Å).*

The fluorescence lifetime of ATTO740-N-terminally labeled horse heart Mb in deoxy and carboxy was calculated by using equation (4.6) (Table 4.12).
The distance from attachment position of dye to the Glycine 1 to the center of the heme (r_P) is 24.2 Å (Figure 4.19A) in the crystal structure of of horse heart Mb (PDB: 1WLA). The linker length to the dye is 11.3 Å (Figure 4.19B) for ATTO 740. All distance measurements were performed in PyMol. For calculation of k_{ET} and E, we assume r = | r_P + r_{Linker} | which is estimated to be 35.5 Å for ATTO 740-labeled horse heart Mb (Figure 4.18).

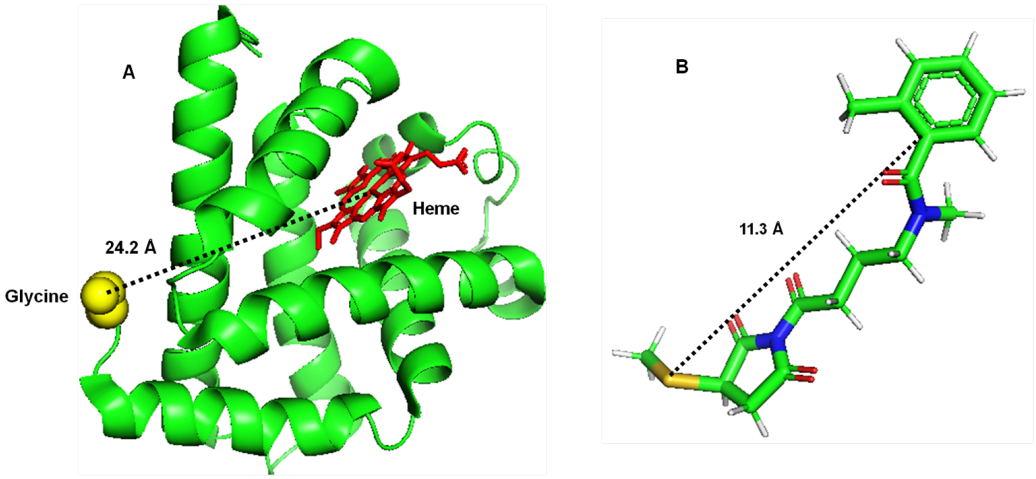

Figure 4.19 *Estimation of the distance between dye and heme based on PyMOL distance calculations. The distance was calculated as the distance from the attachment position of dye on the glycine 1 to the center of the heme (24.2 Å) in horse heart Mb (PDB: 1WLA) plus the linker length to the dye (ATTO 740: 11.3 Å).*

The k_{ET} values were then calculated and the results shown in Table 4.12 for ATTO 643- and Cy7-labeled sperm whale deoxy-Mb, and MbCO, and ATTO 740-labeled horse heart deoxy-Mb, MbCO based on the value of R_0 (Table 4.1), τ_D (lifetime of free dyes as specified by the manufacturer, and in the case of Cy7, the lifetime as specified in literature [19]) and the assumed distances r ($| r_P + r_{Linker} |$) (Figures 4.18A, and 4.19A).
The energy transfer efficiency (*E*) depends on the distance (r) between the donor and acceptor with an inverse 6th-power law due to the dipole–dipole coupling mechanism:

$$E = \frac{1}{1+(\frac{r}{R_0})^6} \qquad 4.5$$

Calculated *E* values for ATTO 643, Cy7, and ATTO 740 dye labeled deoxy-Mb, and MbCO are given in Table 4.12.

4.3.2.3 Calculation of the fluorescence lifetimes of the dyes bound to Mb (τ_{DA})

The lifetime of dyes attached to Mb (τ_{DA}) can be calculated by the following formula:

$$\tau_{DA} = \frac{\tau_D}{1+(\frac{R_0}{r})^6} \qquad 4.6$$

In this formula τ_D, r, and R_0 are the lifetime of the dye in absence of an acceptor, the donor-acceptor distance, and the Förster radius, respectively.
The values of τ_{DA} were calculated for ATTO 643 and Cy7, and ATTO 740 dye labeled deoxy-Mb, MbCO (Table 4.12).

Table 4.12 *Calculated R_0 (Eq 4.1), FRET rate (k_{ET}) (Eq 4.4) and Energy Transfer Efficiency (E) (Eq 4.5), lifetime (Eq 4.6) and experimental lifetime for ATTO 643-, Cy7-, and ATTO 740-deoxy-Mb, and MbCO and lifetimes of corresponding three free dyes.*

Sample	R_0 (nm)	k_{ET} (ns^{-1})	E	Calculated Lifetime[c] (ns)			Experimental Lifetime (ns)
				$r = r_P + r_{Linker}$	$r = r_P$	$r^d = r_P - r_{Linker}$	
ATTO643	-	-	-	-			3.5
ATTO643 - deoxy-Mb[a]	3.54	0.16	0.36	2.24	0.63	0.031	3.54
ATTO643-MbCO[a]	2.46	0.018	0.06	3.29	2.28	0.25	3.30
Cy7	-	-	-	-			0.43
Cy7 - deoxy-Mb[a]	2.99	0.23	0.1	0.39	0.2	0.001	0.84
Cy7 - MbCO[a]	2.00	0.02	0.01	0.43	0.37	0.017	0.81
ATTO 740	-	-	-	-			0.65
ATTO 740 - deoxy-Mb[b]	2.54	0.21	0.11	0.57	0.33	0.01	N.A.
ATTO 740-MbCO[b]	1.66	0.016	0.01	0.64	0.59	0.11	0.87

[a] *Dye labeled-mutated Mb (sperm whale)*
[b] *N-terminus-labeled Mb (Horse Heart)*
[c] *The lifetimes were calculated based on the τ_D that has been reported by the manufacturer except for Cy7 that the lifetime has been used from ref. [19].*
[d] *As mentioned before the hypothesis of* $r = r_P - r_{Linker}$ *in the reality is not true and is ignored, however, the data is reported for comparison to other two calculated r.*

Based on the calculated k_{ET} and E, the energy transfer probability for ATTO 643-labeled deoxy-Mb compared to ATTO 643-labeled-MbCO, is six times more efficient and almost nine times faster while for Cy7 labeled deoxy-Mb compared to Cy7 labeled-MbCO, energy transfer efficiency is ten times faster and k_{ET} is almost twelve times larger. In addition, based on equation 4.4 and 4.5, the calculated k_{ET}, and E values for ATTO 740 labeled deoxy-Mb, and MbCO are: 0.21 ns^{-1}, 0.01 ns^{-1} and, 0.11, 0.01 respectively (Table 4.11), and the calculated k_{ET} and E, the energy transfer for ATTO 740-labeled deoxy-Mb compared to ATTO 740-labeled-MbCO, is around 10 times more efficient and almost 13 times faster, which is approximately similar to what we have calculated for Cy7.

This considerable difference in k_{ET} and E between ATTO 643 and both Cy7 and ATTO 740 is mainly due to the better spectral overlap of the emission of Cy7 and ATTO 740 with the absorption of deoxy-Mb with respect to MbCO than for ATTO 643.
In the case of ATTO 643, the calculated lifetime of the labeled-MbCO is close to the experimentally measured lifetime, however, for the deoxy-Mb form, there is a large difference between calculated and experimental results (Table 4.12). This discrepancy may be due to the significant simplification inherent in the calculated distance, e.g., by the fact that it ignores any orientational effects.
For Cy7 attached to Mb, both forms showed significantly longer lifetimes than those predicted by the calculations, possibly due to the dye attachment on the protein having changed the fluorescent properties of the dye. However, the fact that no significant change in lifetime between the two forms could be observed experimentally is in line with the calculated lifetime differences (Table 4.12).
Regarding the ensemble experimental fluorescence lifetimes of S3C Mb variants, we could not see a difference in lifetime between ATTO 643- and Cy7-labeled deoxy-Mb and -MbCO. However, for ATTO 643- and Cy7-labeled met-Mb, some quenching due to FRET has been observed possibly because of the improved overlap between emission spectra of Cy7 and ATTO 643 dyes with absorption spectrum of met-Mb compared to the other two forms. In the case of deoxy-Mb and MbCO, one possible explanation for this result, is that the dyes have been attached too far away from the heme.
For Cy7, not only the experimental decays show no difference between deoxy-Mb and MbCO but also the highly idealized calculations predict only a relatively small lifetime change. It should be noted that the experimental results showed that binding Cy7 to the Mb is accompanied by a significant change in lifetime (longer) compared to the free dye which is due to the environmental sensitivity of this fluorophore, particularly by limiting dye distortions and conformational fluctuations. The longer lifetime of the dye after attachment to the protein, however, would help us to measure the lifetime more accurately with better resolution.
Interestingly, in the case of ATTO 643, calculations predict a visible effect. The lack of a visible effect in the experimental data may be because the labeling position yields an unfavorable orientation of the dye toward the heme due to steric hindrance, reducing the FRET efficiency. However, it should be pointed out that some quenching effect is visible for met-Mb with both dyes (Table 4.3). Since met-Mb has the largest Förster radius of the three forms, this further points towards a too large of distance, possibly coupled with unfavorable attachment geometry.
Regarding the experimental ensemble fluorescence lifetime of N-terminally labeled Mb, the fluorescence decays of different variants and of the free dye show different intensities. For the met and deoxy forms, the intensity is low, presumably because of fluorescence quenching. However, as expected, the intensity is larger for ATTO 740-labeled MbCO. So the CO form of labeled Mb can be distinguished from the other two forms (deoxy and met forms) on the basis of the fluorescence intensities. The low fluorescent intensity and interference with the IRF (tau~ 0.6 ns) do not allow for sufficiently precise lifetime data.
Comparing calculated values of R_0, k_{ET}, and E for Cy7 and ATTO740 with deoxy-Mb and MbCO shows a difference between the two Mb forms (Table 4.12). But experimentally, for Cy7, the difference between the two forms of Mb could not be distinguished (Figure 4.11) while, for ATTO 740, the two states could be recognized on the basis of the intensity of the fluorescent decay (Figure 4.15). This remarkable difference between ATTO 740 and Cy7 can be connected to the different R_0 values

and how the dyes after labeling interact with the protein and solution, which directly affects the orientation and distance of the dye to the heme center (r), resulting in different quenching.
It is worth mentioning that, although we could not see the difference between the two states in ATTO 643 and Cy7 labeled-deoxy-Mb and -MbCO (Table 4.3), we could see a significant different (based on the fluorescence intensity) for ATTO 740-labeled-deoxy-Mb and -MbCO, which will allow us to monitor these two states in a mixture after illumination of labeled-MbCO with near infra-red light and to study the rebinding kinetics of CO. It might enable successful single molecule-FRET monitoring of CO unbinding and rebinding.
Finally, we should consider that the dyes, after attachment to the protein, may change their spectral properties and even the properties of the protein and that this may affect the FRET efficiencies and the kinetics of binding and rebinding.

4.4 Conclusion

Based on the results of Chapter 3, we concluded that the illumination of MbCO with near infra-red light (700-800 nm) does not break the Mb-CO bond efficiently and we estimated that MbCO will be stable with an upper estimate of dissociation quantum yield less than 6% under illumination with near infra-red light (λ > 700 nm).
We used FRET by which the donor emission is quenched through a non-fluorescent acceptor (the protein heme) that can be used to study the kinetics of CO rebinding. In our experiments, the acceptors are the different states of myoglobin, which exhibit different quenching efficiencies. For example, deoxy-Mb in which CO is unbound from Mb acts as a more efficient quencher than MbCO, where CO is bound to Mb.
In chapter 4, we have labeled MbCO with dyes which emit in the near infra-red (ATTO 740 and Cy7). This enables studies of the energy transfer from the dye to the Mb when illuminating with λ > 700 nm. However, it is essential to be able to distinguish between MbCO and deoxy-Mb when illuminating Mb with near infra-red light. Based on the results of Chapter 4, we could observe a significant difference (based on the fluorescence intensity) for ATTO 740 labeled-deoxy-Mb and -MbCO, which reveals the possibility to distinguish these two states in a mixture. Here, we can use infrared illumination of the labeled-MbCO to study rebinding kinetics of CO to the labeled-deoxy-Mb. These results open a new research area for single molecule-FRET experiments, which is sensitive and specific for labeled molecules and provides useful information about heterogeneity of rates and molecules in an ensemble.

References

(1) Eftink, M. R.; Shastry, M. C. Fluorescence Methods for Studying Kinetics of Protein-Folding Reactions. *Methods Enzymol.* **1997**, *278*, 258–286.

(2) Brown, M. P.; Royer, C. Fluorescence Spectroscopy as a Tool to Investigate Protein Interactions. *Curr. Opin. Biotechnol.* **1997**, *8* (1), 45–49.

(3) Schuler, B. Single-Molecule Fluorescence Spectroscopy of Protein Folding. *ChemPhysChem* **2005**, *6* (7), 1206–1220.

(4) Schuler, B. Single-Molecule FRET of Protein Structure and Dynamics - a Primer. *J. Nanobiotechnology* **2013**, *11* (1), S2.

(5) Pradhan, B.; Engelhard, C.; Mulken, S. V.; Miao, X.; Canters, G. W.; Orrit, M. Single Electron Transfer Events and Dynamical Heterogeneity in the Small Protein Azurin from Pseudomonas Aeruginosa. *Chem. Sci.* **2020**, *11* (3), 763–771.

(6) Cupane, A.; Leone, M.; Vitrano, E.; Cordone, L. Structural and dynamic properties of the heme pocket in myoglobin probed by optical spectroscopy. *Biopolymers* **1988**, *27*(12),1977-1997.

(7) The absorption spectra and extinction coefficients of myoglobin - PubMed https://pubmed.ncbi.nlm.nih.gov/18119239/ (accessed 2022 -04 -01).

(8) Direct observation of ultrafast large-scale dynamics of an enzyme under turnover conditions | PNAS https://www.pnas.org/doi/abs/10.1073/pnas.1720448115 (accessed 2022 -04 -01).

(9) Analysis of Complex Single-Molecule FRET Time Trajectories - ScienceDirect https://www.sciencedirect.com/science/article/pii/S0076687910720115 (accessed 2022 -04 -01).

(10) Somssich, M.; Ma, Q.; Weidtkamp-Peters, S.; Stahl, Y.; Felekyan, S.; Bleckmann, A.; Seidel, C. A. M.; Simon, R. Real-Time Dynamics of Peptide Ligand-Dependent Receptor Complex Formation in Planta. *Sci. Signal.* **2015**, *8* (388), ra76.

(11) Kapusta, P.; Wahl, M.; Benda, A.; Hof, M.; Enderlein, J. Fluorescence Lifetime Correlation Spectroscopy. *J. Fluoresc.* **2007**, *17* (1), 43–48.

(12) Schuler, B. Single-Molecule FRET of Protein Structure and Dynamics - a Primer. *J. Nanobiotechnology* **2013**, *11 Suppl 1*, S2.

(13) Lerner, E.; Barth, A.; Hendrix, J.; Ambrose, B.; Birkedal, V.; Blanchard, S. C.; Börner, R.; Sung Chung, H.; Cordes, T.; Craggs, T. D.; Deniz, A. A.; Diao, J.; Fei, J.; Gonzalez, R. L.; Gopich, I. V.; Ha, T.; Hanke, C. A.; Haran, G.; Hatzakis, N. S.; Hohng, S.; Hong, S.-C.; Hugel, T.; Ingargiola, A.; Joo, C.; Kapanidis, A. N.; Kim, H. D.; Laurence, T.; Lee, N. K.; Lee, T.-H.; Lemke, E. A.; Margeat, E.; Michaelis, J.; Michalet, X.; Myong, S.; Nettels, D.; Peulen, T.-O.; Ploetz, E.; Razvag, Y.; Robb, N. C.; Schuler, B.; Soleimaninejad, H.; Tang, C.; Vafabakhsh, R.; Lamb, D. C.; Seidel, C. A.; Weiss, S. FRET-Based Dynamic Structural Biology: Challenges, Perspectives and an Appeal for Open-Science Practices. *eLife* **2021**, *10*, e60416.

(14) ATTO-TEC GmbH - ATTO-TEC GmbH https://www.atto-tec.com/?language=de (accessed 2022 -04 -01).

(15) Chroma Technology Corp https://www.chroma.com (accessed 2022 -04 -01).

(16) PyMOLWiki https://pymolwiki.org/index.php/Main_Page (accessed 2022 -04 -01).

(17) https://www.jenabioscience.com/images/PDF/PP-305-647N.0002.pdf.

(18) https://www.edinst.com/wp-content/uploads/2017/04/EI_FLS1000_Brochure_Product_02.2022_Stage-02.2.pdf.

(19) Ghann, W.; Kang, H.; Emerson, E.; Oh, J.; Chavez-Gil, T.; Nesbitt, F.; Williams, R.; Uddin, J. Photophysical Properties of Near-IR Cyanine Dyes and Their Application as Photosensitizers in Dye Sensitized Solar Cells. *Inorganica Chim. Acta* **2017**, *467*, 123–131.